Kinetic Analysis of the Slow Ionization of Glutathione by Microsomal Glutathione Transferase MGST1[†]

Ralf Morgenstern,*[,‡] Richard Svensson,[‡] Bryan A. Bernat,[§] and Richard N. Armstrong*[,§]

Institute of Environmental Medicine, Division of Biochemical Toxicology, Karolinska Institutet, Box 210, S-171 77 Stockholm, Sweden, and the Departments of Biochemistry and Chemistry, Center in Molecular Toxicology, Vanderbilt University School of Medicine, Nashville, Tennessee 37232-0146

Received October 5, 2000; Revised Manuscript Received January 9, 2001

ABSTRACT: An important aspect of the catalytic mechanism of microsomal glutathione transferase (MGST1) is the activation of the thiol of bound glutathione (GSH). GSH binding to MGST1 as measured by thiolate anion formation, proton release, and Meisenheimer complex formation is a slow process that can be described by a rapid binding step ($K_d^{GSH} = 47 \pm 7$ mM) of the peptide followed by slow deprotonation ($k_2 = 0.42 \pm 0.03$ s^{-1}). Release of the GSH thiolate anion is very slow (apparent first-order rate $k_{-2} = 0.0006 \pm 0.00002$ s^{-1}) and thus explains the overall tight binding of GSH. It has been known for some time that the turnover (k_{cat}) of MGST1 does not correlate well with the chemical reactivity of the electrophilic substrate. The steady-state kinetic parameters determined for GSH and 1-chloro-2,4-dinitrobenzene (CDNB) are consistent with thiolate anion formation (k_2) being largely rate-determining in enzyme turnover ($k_{cat} = 0.26 \pm 0.07$ s^{-1}). Thus, the chemical step of thiolate addition is not rate-limiting and can be studied as a burst of product formation on reaction of halo-nitroarene electrophiles with the E·GS$^-$ complex. The saturation behavior of the concentration dependence of the product burst with CDNB indicates that the reaction occurs in a two-step process that is characterized by rapid equilibrium binding ($K_d^{CDNB} = 0.53 \pm 0.08$ mM) to the E·GS$^-$ complex and a relatively fast chemical reaction with the thiolate ($k_3 = 500 \pm 40$ s^{-1}). In a series of substrate analogues, it is observed that log k_3 is linearly related (ρ value 3.5 ± 0.3) to second substrate reactivity as described by Hammett σ^- values demonstrating a strong dependence on chemical reactivity that is similar to the nonenzymatic reaction ($\rho = 3.4$). Microsomal glutathione transferase 1 displays the unusual property of being activated by sulfhydryl reagents. When the enzyme is activated by *N*-ethylmaleimide, the rate of thiolate anion formation is greatly enhanced, demonstrating for the first time the specific step that is activated. This result explains earlier observations that the enzyme is activated only with more reactive substrates. Taken together, the observations show that the kinetic mechanism of MGST1 can be described by slow GSH binding/thiolate formation followed by a chemical step that depends on the reactivity of the electrophilic substrate. As the chemical reactivity of the electrophile becomes lower the rate-determining step shifts from thiolate formation to the chemical reaction.

Glutathione (GSH)[1] transferases offer a principal defense against reactive, electrophilic compounds in aerobic organisms. Several families of soluble and membrane-bound proteins display an extremely broad substrate specificity. Three membrane-bound GSH transferases (MGST1, MGST2, and MGST3) have been grouped into a superfamily of proteins named MAPEG (*m*embrane *a*ssociated *p*roteins in *e*icosanoid and *G*SH metabolism) also containing 5-lipoxygenase activating protein, leukotriene C_4 synthase, and the newly discovered GSH dependent prostaglandin E synthase (*1*, *2*). The latter is actually the closest relative of MGST1 (38% amino acid sequence identity), which is the enzyme that has been studied in most detail to date. Common to all of these enzymes is the interaction with fatty acid derivatives. The interactions though vary from binding, epoxide conjugation, hydroperoxide GSH peroxidase mediated reduction to GSH dependent oxidoreduction of an endoperoxide. The MAPEG superfamily thus plays an important role in transformations of reactive oxygenated fatty acids (and phospholipids) that are formed either in the production of important physiological mediators or during oxidative stress. Although soluble and membrane-bound glutathione transferases are not related with respect to structure and evolutionary origin, they do display extensive functional overlap (*3*, *4*).

Electron crystallography of two-dimensional crystals and other biochemical investigations of MGST1 indicate that the protein is a homotrimer with subunits 17 kDa in molecular

[†] Supported by the Swedish Cancer Society, The Swedish National Board for Laboratory Animals, Carl Tryggers Foundation, funds from Karolinska Insitutet, and NIH Grants R01 GM30910, P30 ES00267, and T32 ES07028 from the National Institutes of Health.

* Address correspondence to these authors. E-mail: ralf.morgenstern@imm.ki.se; r.armstrong@vanderbilt.edu; phone/fax: +4687287574/+468343846.

[‡] Karolinska Institutet.

[§] Vanderbilt University.

[1] Abbreviations: GSH, glutathione; CDNB, 1-chloro-2,4-dinitrobenzene; CNAP, 4-chloro-3-nitroacetophenone; CNBAM, 4-chloro-3-nitrobenzamide; 2,5-DCNB, 2,5-dichloronitrobenzene; TNB, 1,3,5-trinitrobenzene; NEM, *N*-ethylmaleimide; EDTA, ethylenediamine tetraacetic acid.

10.1021/bi0023394 CCC: $20.00
Published on Web 02/21/2001

mass (*5*−*7*). Equilibrium binding studies suggest that only a single molecule of GSH is bound to the trimer (*8*). It is not clear if the enzyme has three active sites per trimer and functions with one-third-the-sites-reactivity or if the trimer forms three symmetry related but mutually exclusive binding modes at a single active site.

The chemical mechanism of GSH transferases involves the enzyme-assisted ionization of GSH to the more reactive thiolate anion. The chemical and kinetic features of the ionization of enzyme-bound GSH by the canonical soluble enzymes are relatively well understood (*3*, *9*, *10*). The mechanism of action of the microsomal enzyme, however, has remained an enigma. One unique aspect of the microsomal enzyme is its activation by sulfhydryl reagents such as *N*-ethyl maleimide, NEM. The exact step that is altered in activation has not been elucidated, although GSH binding has been implicated (*11*).

In this paper, we report the unusually slow ionization of GSH upon binding to microsomal GSH transferase MGST1. Kinetic measurements of thiolate formation, proton release, and presteady-state reactions with 1-chloro-2,4-dinitrobenzene and 1,3,5-trinitrobenzene at 4 °C are consistent with a rapid equilibrium binding of the peptide $K_d^{GSH} \approx 50$ mM followed by a slow conformational transition of the protein $k \approx 0.5$ s^{-1} leading to thiolate formation. The amplitudes of all these measurements indicate a stoichiometry of one GSH molecule bound per homotrimer. The measured off rate for the bound thiolate is exceedingly slow with a half-life of about 20 min. Reaction of the enzyme-bound thiolate with many electrophilic substrates is quite rapid indicating that thiolate formation often limits the rate of enzyme turnover. When the enzyme is activated by *N*-ethylmaleimide, the rate of thiolate anion formation is greatly enhanced, demonstrating for the first time the specific step that is altered by NEM modification.

MATERIALS AND METHODS

Chemicals. 1-Chloro-2,4-dinitrobenzene was obtained from Merck Co. (Darmstadt, Germany). 4-Chloro-3-nitroacetophenone and 2,5-dichloronitrobenzene were from Aldrich-Chemie (Steinheim, Germany). 4-Chloro-3-nitrobenzamide was from Alfred Bader Library of Rare Chemicals, Division of Aldrich Chemical Co. (Milwaukee, WI). Glutathione and *N*-ethylmaleimide were from Sigma Chemical Co. (St. Louis, MO). Bromocresol purple was from (Fluka Chemie AG, Buchs, Switzerland). 1,3,5-Trinitrobenzene was a generous gift from Nobel-Chemistry (Karlskoga, Sweden). All other chemicals were of reagent grade and obtained from common commercial sources.

Enzyme Preparation. MGST1 was purified from rat liver as previously described (*12*). To decrease the interference from the absorbance of Triton X-100, a 0.2% rather than 1.0% detergent concentration was used in the last purification step. Preparation of the enzyme for stop-flow experiments involved buffer exchange, and GSH removal was done on 10 DG gel filtration columns (Bio-Rad Laboratories) according to the manufacturer's instructions. Buffers used were 0.1 M potassium phosphate (pH 7.0) containing 20% glycerol, 0.1 mM EDTA, 0.2% Triton X-100 (buffer A) or 80 mM NaCl, 0.08 mM EDTA, 20% glycerol, 0.2% Triton X-100, and 10 μM bromocresol purple (pH 7.0) (buffer B). Protein concentration was determined as described by Peterson (*13*) with bovine serum albumin as the standard, a procedure that has previously been shown to yield accurate values when calibrated against amino acid analysis.

Stopped-Flow Experiments. Applied Photophysics stopped-flow instruments equipped with either one or two monochromators were used for all experiments. Between 50 and 100 μL from each of two syringes was rapidly mixed in the 10-mm path length cell if not otherwise indicated, and the signal was recorded. In general, three-trace averages were used to fit theoretical expressions describing either a single exponential or, where appropriate, a single exponential followed by a steady state. All experiments were performed at 4−6 °C. All concentrations given below are the resulting final concentrations in the observation cell. The enzyme concentration is expressed as the concentration of subunits.

GSH Binding and Thiolate Anion Formation. Enzyme (10−50 μM) in buffer A was rapidly mixed with the same buffer containing 0.15 to 100 mM GSH. The appearance of absorbance at 239 nm was followed and fitted to a single exponential with the software provided ($\epsilon_{239} = 5000$ M^{-1} cm^{-1}). An optical path length of 10 mm was used except with 50 and 100 mM GSH where a 2-mm cell was employed to mitigate for the high background absorbance of GSH.

GSH Release. GSH release was followed at 239 nm by mixing 35 μM purified enzyme containing 1 mM GSH with 10 or 20 mM glutathione sulfonate at pH 7.0 (*14*). The absorbance decrease was recorded on a Philips PU8720 spectrophotometer, and the data were fitted to a single exponential by the program Graphpad Prism 3.

GSH Binding and Proton Release. Enzyme (40−50 μM) in buffer B (pH 7.0) was rapidly mixed with the same buffer containing 1 to 100 mM GSH (pH 7.0). The change in pH was followed as an absorbance decrease in bromocresol purple at 588 nm and was fitted to a single exponential with the software provided. Independent experiments to obtain the stoichiometry of proton release were performed where 1 mM NaOH was used to titrate back to the original absorbance obtained just after GSH addition. In the potentiometric measurements, enzyme (120 μM) in buffer B was mixed with 1 mM GSH. Again, 1 mM NaOH was used to titrate back to the original pH. No interference by CO_2 within the experimental time was detected.

Meisenheimer Complex Formation. Enzyme in buffer A containing 0.4 mM 1,3,5-trinitrobenzene was rapidly mixed with the same buffer containing between 0.5 and 100 mM GSH. The formation of the dead-end Meisenheimer complex stabilized by the enzyme was recorded at 450 nm (*15*, *16*).

Presteady-State Kinetics. Enzyme in buffer A containing 0.5 mM GSH was rapidly mixed with buffer A containing CDNB, and the burst of product formation was recorded at 340 nm, $\Delta\epsilon = 9600$ M^{-1} cm^{-1}. Alternatively, CDNB analogues were used and appropriate wavelengths were selected: 4-chloro 3-nitroacetophenone (CNAP, $\Delta\epsilon_{297} = 11\,900$ M^{-1} cm^{-1}), 4-chloro 3-nitrobenzamide (CNBAM, $\Delta\epsilon_{370} = 3100$ M^{-1} cm^{-1}), 2,5-dichloronitrobenzene (2,5-DCNB, $\Delta\epsilon_{383} = 700$ M^{-1} cm^{-1}).

Steady-State Kinetics. Kinetic parameters of MGST1 were determined at an assay temperature of 5 °C in buffer A, and GSH was varied between 0.1 and 25 mM at 0.5 mM CDNB. CDNB was varied between 1 μM and 0.5 mM at 10 mM GSH. Duplicate and triplicate determinations were per-

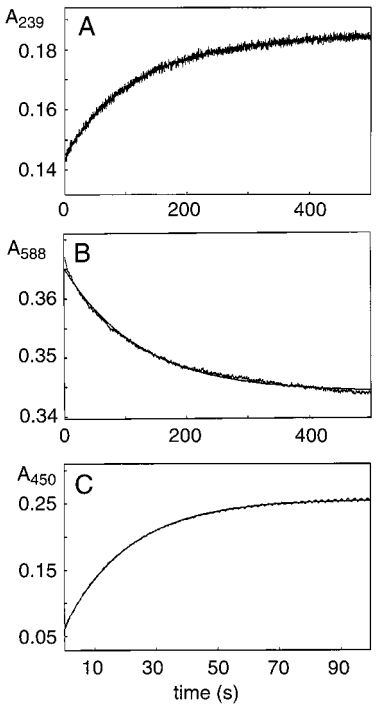

FIGURE 1: Kinetics of E·GS$^-$ formation at 4 °C. (A) Increase in A_{239} on mixing MGST1 (22 μM monomer) with 1 mM GSH. The solid line is a fit to a single exponential with $k_{obs} = (8.33 \pm 0.05) \times 10^{-3}$ s^{-1}. (B) Proton release monitored with bromcresol purple at 588 nm on mixing MGST1 (43 μM monomer) with 1 mM GSH. The solid line is a fit of the data to a single exponential with $k_{obs} = (8.04 \pm 0.05) \times 10^{-3}$ s^{-1}. (C) σ-Complex formation monitored at 450 nm on mixing MGST1 (30.0 μM monomer) containing 0.4 mM TNB with 5.0 mM GSH. The solid line is a fit to a single exponential with $k_{obs} = (4.47 \pm 0.01) \times 10^{-2}$ s^{-1}.

formed. Kinetic parameters were derived by nonlinear regression using the program package Graphpad Prism 3.

RESULTS

Thiolate Anion Formation, A Slow Two-Step Process. Rapid mixing of MGST1 with GSH results in an increase in absorbance at 239 nm that can be fit to a single exponential (Figure 1, panel A). The concentration dependence of k_{obs} for thiolate formation exhibits saturation behavior as illustrated in Figure 2, panel A. It is evident from Figure 1, panel A, that thiolate anion formation is a slow process indeed. This kinetic behavior is consistent with a two-step mechanism, illustrated in eq 1, involving a rapid equilibrium formation of an initial complex ($K_d^{GSH} = 47$ mM) followed by the slow appearance of the enzyme-bound thiolate. Under

$$E + GSH \underset{k_{-1}}{\overset{k_1}{\rightleftharpoons}} E{\cdot}GSH \underset{k_{-2}}{\overset{k_2}{\rightleftharpoons}} E^*{\cdot}GS^- + H^+ \qquad (1)$$

$$k_{obs} = k_{-2} + \frac{k_2[GSH]}{K_d^{GSH} + [GSH]} \quad \text{where} \quad K_d^{GSH} = k_{-1}/k_1 \qquad (2)$$

favorable conditions, the dissociation constant and rate constants k_2 and k_{-2} can be obtained from the dependence of k_{obs} on [GSH] (eq 2). The kinetic constants are shown in Table 1. Whereas, the K_d^{GSH} and k_2 describing the deprotonation step can be determined with good precision, k_{-2} for thiolate anion protonation (or GS$^-$ release), is too small to be well-defined by extrapolation to [GSH] = 0. If it is

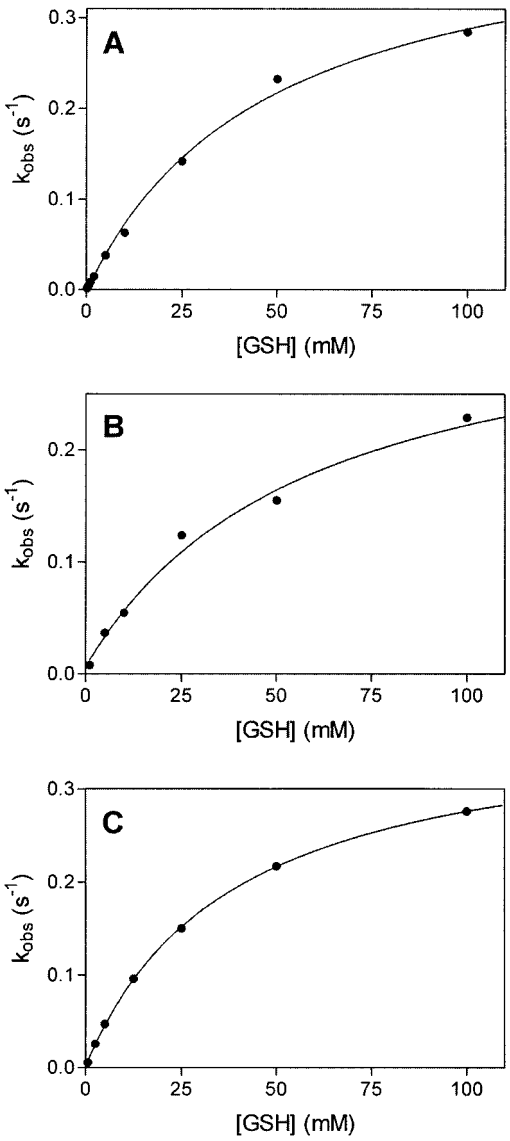

FIGURE 2: Dependence of k_{obs} on [GSH] for (A) Thiolate formation at 239 nm; (B) Proton release by monitored with bromcresol purple; and (C) σ-Complex formation with TNB. The solid lines are best fits of the data to eq 2 with the rate and equilibrium constants listed in Table 1.

Table 1: Kinetic Constants for Thiolate Anion Formation on Mixing MGST1 with GSH

experiment	K_d (mM)	k_2 (s^{-1})	k_{-2} (s^{-1})
thiolate formation	47 ± 7	0.42 ± 0.03	0.000 ± 0.004
proton release	55 ± 21	0.34 ± 0.05	0.006 ± 0.012
σ-complex formation	38 ± 1	0.38 ± 0.04	0.002 ± 0.001
GS$^-$ release			0.0006 ± 0.00003

assumed that the ϵ_{239} for E·GS$^-$ is similar to that of other thiolate anions (ca. 5000 M^{-1} cm^{-1}), then the amplitude of the signal is consistent with a single thiolate formed per homotrimer.

Independent measurements of thiolate anion formation can be obtained by observing proton release from the E·GSH complex and by rapid reaction of the E·GS$^-$ complex with 1,3,5-trinitrobenzene. The [GSH] dependence of the kinetics of proton release, as measured by the pH indicator bromocresol purple at 588 nm in the stopped flow (Figures 1B and 2B), mirrored that of thiolate anion formation observed at 239 nm discussed above. It is important to note that the

Chart 1

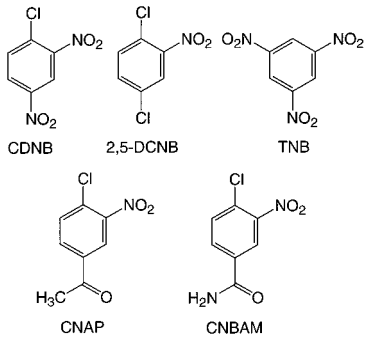

rate constant for proton release is identical to that for thiolate formation but determined in the absence of buffer. This fact suggests that there is no detectable buffer catalysis of proton transfer under the conditions of these particular experiments. The stoichiometry of proton release was determined independently by potentiometric titration. When unbuffered solutions of enzyme and GSH (pH 7.0) were mixed, the resulting solution required the addition 1.05 ± 0.06 equiv of KOH/trimer to return the solution to the original pH. Thus, one proton was released per trimer upon binding GSH.

Finally, it is known that 1,3,5-trinitrobenzene (TNB, Chart 1) reacts rapidly and reversibly with thiolate anions to form a Meisenheimer complex (*15*, *16*) which absorbs at 450 nm. When enzyme, preincubated with TNB, is rapidly mixed with GSH, Meisenheimer complex formation (Figures 1C and 2C) is slow and occurs at a rate equivalent to that seen for thiolate formation and proton release (Table 1). It can be concluded that the ionization of E·GSH is slow and constitutes the rate-limiting step in Meisenheimer complex formation.

In an effort to obtain a more accurate measure of k_{-2} in eq 1, an independent measurement of thiolate anion protonation (or GS^- release) was made by analyzing the rate of GS^- loss from E·GS^- when the complex is rapidly mixed with an excess of the inhibitor, glutathione sulfonate (K_d = 10 μM). The release was measured by following the decrease in absorbance at 239 nm. The data (Figure 3) could be fitted to a single exponential providing a more precise determination of k_{-2} (Table 1). The rate constant for loss of thiolate was independent of the concentration of the inhibitor when [GSO_3^-] ≥ 10 mM. GSH binding can thus be described as consisting of a rapid step where the substrate is bound with low affinity (K_d = 47 mM), while subsequent thiolate anion

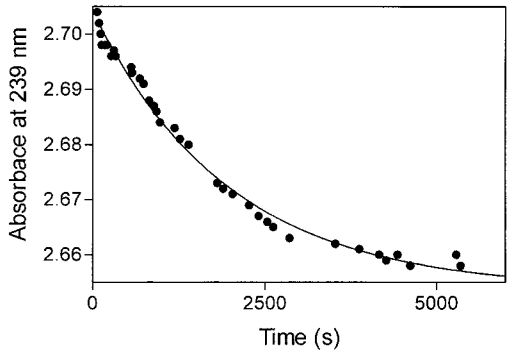

FIGURE 3: Loss of thiolate absorbance at 239 nm on mixing E·GS^- (37 μM monomer containing 1 mM GSH) with 10 mM glutathione sulfonate. The experimental points were fitted to a single-exponential decay (solid line) with a rate constant of 0.0006 ± 0.00003 s^{-1}.

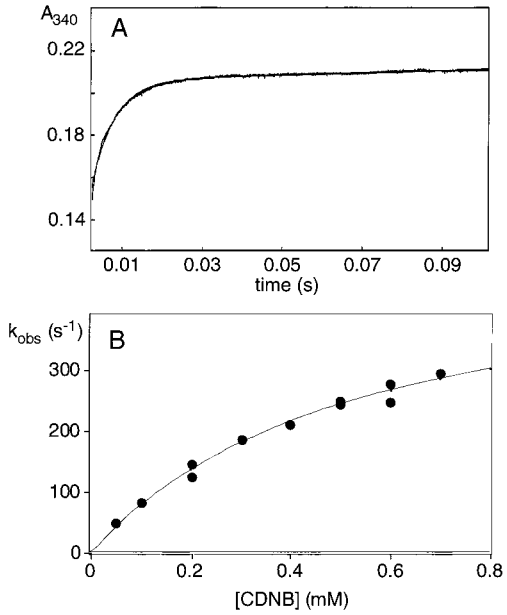

FIGURE 4: Pre-steady-state kinetics of the reaction of CDNB with E·GS^- complex. (A) Burst of product formation monitored at 340 nm on mixing a solution of enzyme and GSH with a solution of CDNB. Final concentrations were 17 μM enzyme, 1 mM GSH, and 0.2 mM CDNB. The observed rate constant for the burst of product formation was 175 ± 1 s^{-1}. (B) Dependence of k_{obs} for the burst on [CDNB] at [GSH] = 0.5 mM. The solid line is regression fit of the data to eq 4 with K_d^E = 0.53 ± 0.08 mM and k_3 = 510 ± 40 s^{-1}.

formation is slow. Once the thiolate is formed, release or reprotonation is very slow indeed. The overall dissociation constant for GS^- can be calculated from the individual rate and equilibrium constants for the linked equilibria of eq 1. The calculated K_d is 70 ± 30 μM and is in reasonable agreement with 20 μM obtained experimentally from equilibrium dialysis (*8*). The amplitudes of thiolate anion formation are consistent with earlier observations that each homotrimer binds approximately one (1.2 ± 0.06) GSH molecule.

Electrophilic Substrate Binding and Catalysis, A Rapid Two-Step Process. To assess the chemical step in catalysis, the presteady-state kinetics of reaction of a series of electrophilic substrates with the preformed E·GS^- complex were determined. Rapid mixing of the E·GS^- complex with CDNB results in a burst of product formation followed by a much slower steady-state rate (Figure 4, panel A). It is clear that the chemical step is rapid in comparison to some step or steps following product formation. The concentration dependence of k_{obs} (Figure 4, panel B) was found to display saturation behavior indicating a two-step process (eq 3) with a rapid-reversible binding step and, in the case of CDNB, a fast chemical step. Since it is known that the chemical reaction is essentially irreversible the data were fitted to eq 4 yielding the dissociation constant of the electrophile (K_d^E)

$$E^*\cdot GS^- + CDNB \overset{K_d^E}{\rightleftharpoons} E^*\cdot GS^-\cdot CDNB \xrightarrow{k_3} E + GSDNB \quad (3)$$

$$k_{obs} = \frac{k_3[CDNB]}{K_d^E + [CDNB]} \quad (4)$$

Table 2: Kinetic Constants for the Reaction of Electrophilic Substrates with the E·GS$^-$ Complex

substrate	K_d^E (mM)	k_3 (s^{-1})
CDNB	0.53 ± 0.08	510 ± 40
CNAP	1.1 ± 0.60	15 ± 6
CNBAM	0.6 ± 0.1	1.0 ± 0.1
2,5-DCNB	0.08 ± 0.03	0.14 ± 0.01

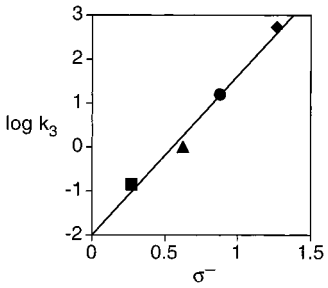

FIGURE 5: Hammett plot of log k_3 vs the substituent constant σ^- for the electrophilic substrates; CDNB (◆), CNAP (●), CNBAM (▲), and 2,5-DCNB (■). The line is a least-squares fit of the data to the equation $\log k_3 = \log k_0 + \rho\sigma^-$ with $\rho = 3.5 \pm 0.3$.

Table 3: Steady State Kinetic Parameters of MGST1 Obtained at 5 °C

substrate	K_M (mM)	k_{cat} (s^{-1})	k_{cat}/K_M ($M^{-1}\,s^{-1}$)
GSH	3.0 ± 0.7	0.26 ± 0.07	86 ± 21
CDNB	0.011 ± 0.002	0.14 ± 0.01	$(1.3 \pm 0.2) \times 10^4$

and the rate constant (k_3) for the chemical reaction. In fact, these measurements give the first estimate of the binding affinity of CNDB to MGST1 (Table 2).

The sensitivity of the chemical reaction step to the reactivity of the substrate was probed in a systematic fashion utilizing electron deficient aryl substrates with different substituents para to the leaving group (Table 2). Of the substrates tested, 2,5-DCNB, the most hydrophobic, displayed the lowest K_d^E. When the logarithm of the obtained chemical rate constants are plotted against the Hammett σ^- substituent constants (Hammett plot), a linear relationship is obtained (Figure 5). The slope (or ρ value) of 3.5 ± 0.3 signifies a strong dependence on reactivity clearly showing that k_3 represents the chemical step. In addition, the ρ value is quite similar to that found for the nonenzymatic (specific-base catalyzed) reaction ($\rho = 3.4$) (*17*). The amplitudes of product formation transients with CDNB indicate that the MGST1 homotrimer harbors approximately one active site (1.44 ± 0.06 equiv of product per trimer).

Steady-State Kinetic Parameters. The burst of product formation followed by a slow steady-state rate observed above is also consistent with a mechanism in which product release is the rate-limiting step. The presteady-state kinetic parameters (Tables 1 and 2) were all obtained at 4−5 °C. Therefore, a set of steady-state kinetic parameters for CDNB and GSH were also determined at this temperature (Table 3). The similarity of k_2 and k_{cat} (0.42 and 0.26 s^{-1}, respectively) indicates that, for reactive substrates, thiolate formation is the rate-limiting step.

Properties of the NEM-Activated Enzyme. When GSH was mixed with NEM-activated enzyme, thiolate formation was found to be much more rapid (Figure 6) than that observed for the unactivated enzyme under the same conditions (Figure 1, panel A). The kinetics of thiolate formation with the activated enzyme are more complex and follow a double exponential. About two-thirds of the signal amplitude is associated with the fast phase. However, the total amplitude of the signal (fast plus slow phase) remains consistent with a stoichiometry of one thiolate formed per trimer. It is also important to note that the rate constants for both phases of the reaction are significantly larger than the rate constant measured with the unactivated enzyme. The burst kinetics of product formation with CDNB in the activated E·GS$^-$ complex are not affected (data not shown). This clearly suggests that the NEM modification enhances catalysis by increasing the rate of thiolate formation rather than affecting some other aspect of the mechanism.

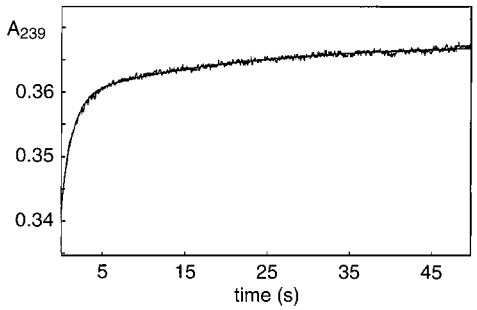

FIGURE 6: Thiolate formation monitored at 239 nm on mixing NEM-activated MGST1 with GSH at 5 °C. The final concentration of enzyme and GSH were 18 μM and 1 mM, respectively. The experimental data were fit to a double exponential with $k_{obs1} = 0.76 \pm 0.01\ s^{-1}$ (amplitude = 0.018) and $k_{obs2} = 0.050 \pm 0.001\ s^{-1}$ (amplitude = 0.0082).

DISCUSSION

Kinetics and Stoichiometry of Thiolate Formation. The catalytic mechanisms of most GSH transferases involve the formation of the enzyme-bound thiolate of GSH (*3*). Although the rate of thiolate formation varies considerably among different GSH transferases, it is usually relatively rapid as compared to turnover (*14*, *18*, *19*). What is unusual about MGST1 is how slowly the thiolate is formed. It seems unlikely that the actual transfer of the proton from the enzyme-bound thiol is so slow. It is more likely that the proton-transfer itself is rapid but is preceded by an obligatory, slow conformational transition. The equilibrium constant for this transition with loss of the proton (eq 1) favors the thiolate species by a factor of about 700 (k_2/k_{-2}). As the microscopic ionization steps for protonation and deprotonation are often very rapid, we suggest that a slow conformational transition limits thiolate anion formation and concomitant proton release in MGST1. Another protein that exhibits relatively slow proton release, bacteriorhodopsin, completes one turnover in 50 ms. Here, conformational transitions are also believed to contribute to individual steps involving vectorial proton transfer (*20*).

Taken together all the measurements of binding stoichiometry obtained here are consistent with earlier equilibrium binding data (*8*). The results provide no evidence for the existence of additional low affinity binding sites for GSH that confer thiolate anion stabilization, which could not be excluded in earlier work. In principle, it is impossible to rule out inactive enzyme in a preparation that would account for substoichiometric thiolate formation as well as substoichio-

metric bursts of product formation in the presteady state. Nevertheless, the consistent results shown here and elsewhere (*8*) and obtained with many different enzyme preparations and in different laboratories argue that MGST1 utilizes only one catalytic site per trimer.

There are two structural possibilities consistent with this one-third-the-sites-reactivity behavior. One is that there are three distinct GSH binding sites in the homotrimer but occupancy of one prevents, through a conformational transition, binding to the others (full negative cooperativity). Recent observations that subunit interactions relating activation of the enzyme to the extent of sulfhydryl reagent modification clearly suggests that the subunits communicate in the trimer (*21*). The second possibility is a single active site in the trimer with three symmetry-related, mutually exclusive binding modes for GSH. The ongoing structural investigations of MGST1 (*22*) have led to a three-dimensional electron density map of the enzyme at a resolution of 6 Å (*23*). A higher resolution structure is anticipated to reveal which of the two above possibilities is the most likely to be correct.

Catalysis and Activation. One curious feature of catalysis by MGST1, noted some time ago (*24*), is the lack of correlation between the steady-state kinetic parameter k_{cat} and the chemical reactivity of the electrophilic substrates. This fact led to the conclusion that a step or steps in the kinetic mechanism other than the chemical one was rate-limiting in certain circumstances. Earlier results have suggested that product release is not rate-limiting for the enzyme-catalyzed reaction between CDNB and GSH (*11*). The results presented here suggest that the slow formation of the enzyme-bound thiolate is the rate-limiting step in turnover of very reactive electrophilic substrates and accounts for the burst of product formation. The concentration dependence of product formation was found to display saturation behavior. Thus, dissociation constants for the second substrates could be derived that indicate a modest binding affinity for the three more reactive compounds (Table 2). The more pronounced hydrophobic character of 2,5-DCNB and the known preference of MGST1 for certain polyhalogenated substrates are consistent with the higher affinity for the latter. As would be predicted for the chemical step log k_3 values are strongly dependent on second substrate reactivity as is evident in the Hammett plot (Figure 5). The dependence is also similar to that of k_{cat}/K_M^E determined earlier (*24*), as would be expected.

Inasmuch as the substrates span several orders of magnitude in chemical reactivity, they can be used to specifically probe the enzyme-catalyzed reaction limited by either thiolate anion formation or chemistry. This point is particularly relevant for dissecting the underlying mechanism of activation of the enzyme by sulfhydryl reagents. It has been suggested that the critical step for which the rate does increase could involve GSH binding (*11*). Indeed, it is shown here that thiolate anion formation is much more rapid in the NEM-activated enzyme. It then follows that for electrophilic substrates where the chemical step is fast, NEM treatment of MGST1 should lead to enhanced turnover or activation. This is indeed the case with CDNB and CNAP. These experiments thus provide the first detailed rationale explaining why the activity of the enzyme toward some substrates but not others is increased upon NEM-treatment of MGST1. 2,5-DCNB and CNBAM are examples of MGST1 substrates where k_3 is comparable to k_2. In this case, k_{cat} is limited also by the chemical reaction, and activation is not observed. However, as would be predicted, when the concentration of GSH is lowered making thiolate anion formation once again rate limiting, activation can be observed with less reactive substrates as well (*11*).

It is important to point out that sulfhydryl reagents also activate the enzyme in the environment of the microsome. Thus, the enhanced turnover is not due to a specific effect of detergent on the conformational dynamics of the purified enzyme. In addition, activation is known to occur in vivo (*25*) and clearly yields a more efficient enzyme. Whether the activated enzyme actually makes a difference in terms of protection under toxic conditions remains to be demonstrated.

If the slow appearance of thiolate is due to a slow conformational transition prior to proton release, then it would appear that NEM modification enhances the rate at which this transition occurs. The more complex kinetics of thiolate formation may be due to heterogeneity in the chemically modified enzyme or a more fundamental aspect of how the subunits in the trimer interact. In any event, it is important to note that both phases of thiolate formation are faster than that observed in the unactivated enzyme. Future studies aimed at describing the detailed properties of the activated enzyme could therefore yield information on additional steps in the GSH binding mechanism not measurable in the unactivated enzyme.

Steady-State Kinetics. That thiolate formation is so slow has interesting consequences for the steady-state kinetics of MGST1. The turnover number, k_{cat}, for chemically reactive substrates is limited by the kinetics of thiolate formation. This fact explains the relative insensitivity of k_{cat} to the reactivity of electrophilic substrates noted earlier (*24*). The K_M values for substrates are also influenced. For example, the K_M value for CDNB is much lower than its apparent dissociation constant from the enzyme. In addition, less reactive electrophiles display a trend toward higher K_M values that approach their actual dissociation constant (*24*). This behavior is expected when an intermediate (free enzyme in this case) accumulates after the chemical step. The K_M value for GSH, on the other hand, is much higher than its true dissociation constant with reactive substrates since the binding does not come to equilibrium. Again the K_M for GSH would tend toward the true dissociation constant as the chemical reaction becomes slower, a trend indeed observed in earlier work (*11*).

Conclusions. These studies reveal that MGST1 displays very slow GSH thiolate anion formation that appears to be the rate-limiting step in the turnover of reactive electrophilic substrates. This step is also now identified as being activated when MGST1 is treated with sulfhydryl reagents. The kinetic analysis of the chemical step provides the mechanistic basis for the previous observation that the steady state rate of only certain (more reactive) second substrates increases when the enzyme is activated by NEM. Further investigation of the activated enzyme is underway.

REFERENCES

1. Jakobsson. P.-J., Morgenstern, R., Mancini, J., Ford-Hutchinson, A., and Persson, B. (1999) *Protein Sci. 8*, 689−692.
2. Jakobsson, P. J., Thoren, S., Morgenstern, R., and Samuelsson, B. (1999*) Proc. Natl. Acad. Sci. U.S.A.* 96, 7220−7225.
3. Armstrong, R. N. (1997) *Chem. Res. Toxicol. 10*, 2−18.
4. Andersson, C., Mosialou, E., Weinander, R., and Morgenstern, R. (1994) in *Conjugation-Dependent Carcinogenicity and Toxicity of Foreign Compounds* (Anders, M. W., Dekant, W., Eds.) pp 19−35, Academic Press, San Diego.
5. Hebert, H., Schmidt-Krey, I., and Morgenstern, R. (1995) *EMBO J. 14*, 3864−3869.
6. Hebert, H., Schmidt-Krey, I., Morgenstern, R., Murata, K., Mitsuoka, K., and Fujiyoshi, Y. (1997) *J. Mol. Biol. 271*, 751−758.
7. Lundqvist, G., Yucel-Lindberg, T., and Morgenstern, R. (1992) *Biochim. Biophys. Acta 1159*, 103−108.
8. Sun, T.-H., and Morgenstern, R. (1997) *Biochem. J. 326*, 193−196.
9. Liu, S., Zhang, P., Ji, X., Johnson, W. W., Gilliland, G. L., and Armstrong, R. N. (1992) *J. Biol. Chem. 267*, 4296−4299.
10. Parsons, J. F., and Armstrong, R. N. (1996) *J. Am. Chem. Soc. 118*, 2295−2296.
11. Andersson, C., Piemonte, F., Mosialou, E., Weinander, R., Sun, T.-H., Lundqvist, G., Adang, A. E. P., and Morgenstern, R. (1995) *Biochim. Biophys. Acta 1247*, 277−283.
12. Morgenstern, R., and DePierre, J. W. (1983) *Eur. J. Biochem. 134*, 591−597.
13. Peterson, G. L. (1977) *Anal. Biochem. 83*, 346−356.
14. Parsons, J. F., Xiao, G., Gilliland, G. L., and Armstrong, R. N. (1998) *Biochemistry 37*, 6286−6294.
15. Graminski, G. F., Zhang, P., Sesay, M. A., Ammon, H. L., and Armstrong, R. N. (1989) *Biochemistry 28*, 6252−6258.
16. Andersson, C., and Morgenstern, R. (1990) *Biochem. J. 272*, 479−484.
17. Chen, W.-J., Graminski, G. F., and Armstrong, R. N. (1988) *Biochemistry 27*, 647−654.
18. Caccuri, A. M., Lo Bello, M., Nuccetelli, M., Nicotra, M., Rossi, P., Federici, G., and Ricci, G. (1998) *Biochemistry 37*, 3028−3034.
19. Jemth, P., and Mannervik, B. (1999) *Biochemistry 38*, 9982−9991.
20. Balashov, S. P. (2000) *Biochim. Biophys. Acta 1460*, 75−94.
21. Svensson, R., Rinaldi, R., Swedmark, S., and Morgenstern, R. (2000) *Biochemistry 39*, 15144−15149.
22. Schmidt-Krey, I., Murata, K., Hirai, T., Mitsuoka, K., Cheng, Y., Morgenstern, R., Fujiyoshi, Y., and Hebert, H. (1999) *J. Mol. Biol.* 288, 243−53.
23. Schmidt-Krey, I., Mitsuoka, K., Hirai, T., Murata, K., Cheng, Y., Fujiyoshi, Y., Morgenstern, R., and Hebert, H. (2000) *EMBO J. 19*, 6311−6316.
24. Morgenstern, R., Lundqvist, G., Hancock, V., and DePierre, J. W. (1988) *J. Biol. Chem. 263*, 6671−6675.
25. Yonamine, M., Aniya, Y., Yokomakura, T., Koyama, T., Nagamine, T., and Nakanishi, H. (1996) *Jpn. J. Pharmacol. 72*, 175−181.

BI0023394